

Magnetic and Geochemical Studies of Iron sand Deposits around Tambora Volcano in Sumbawa, Indonesia: A proxy for search high quality iron sand

Rudarsko-geološko-naftni zbornik (The Mining-Geology-Petroleum Engineering Bulletin) DOI: 10.17794/rgn.2025.5.2

Original scientific paper



Putu Billy Suryanata¹* o ≅, Adella Ulyandana Jayatri² o ≅, Satria Bijaksana¹ o ≅, Silvia Jannatul Fajar¹ (□) □, Ulvienin Harlianti¹ (□) □

- ¹ Faculty of Mining and Petroleum Engineering, Institut Teknologi Bandung, Jalan Ganesa 10, Bandung 40132, Indonesia.
- ² Faculty of Mathematics and Natural Science, Universitas Mataram, Jalan Majapahit 62, Mataram 83125, Indonesia.

Abstract

Tambora Volcano is known as a volcano that had a catastrophic eruption in 1815, with an enormous amount of material released, including pyroclastic flows and fall deposits. From these volcanic products, erosion and transportation processes acted towards the coastline and formed iron sand, which contains economically valuable minerals such as magnetite. Iron sand is one of the important elements/components for the production of steel and titanium, but its use is still limited. In Indonesia, iron sand has only been mined and used as a mixture in the production of cement and building materials because of its low iron content (45-48%). Therefore, it is important to know the characteristics and content of iron sand to maximise the results of iron sand mining. The characteristics of iron sand deposits from Mount Tambora are still unclear and have never been studied. Therefore, we conducted a study to identify the geochemical characteristics and magnetic properties of iron sand around Tambora Volcano to determine the concentration of economic elements from different volcanic products. This study uses magnetic susceptibility measurements, X-Ray Diffraction (XRD), X-Ray Fluorescence (XRF), and Inductively Coupled Plasma - Optical Emission Spectrometry (ICP-OES) measurements. Sampling was carried out at three locations in the area, namely Nanga Miro, Baringin Jaya, and Hodo. The Nanga Miro and Baringin Jaya areas are the lava flow deposit zones of the 1815 eruption and lava flows from previous eruptions, while the Hodo area is just the pyroclastic flow zone of the 1815 eruption. The results showed that the distribution of sand grain sizes in Baringin Jaya and Nanga Miro that are from the lava flow deposit zones are dominantly medium sized (MS) and fine sized (FS). Meanwhile, in Hodo, which is from the pyroclastic flow deposit zone, it is dominantly coarse sized (CS) and medium sized (MS). Areas from the lava flow zones have high susceptibility values, high Fe concentrations, and magnetic mineral content of magnetite and haematite. In addition, the REE elements (Ce, Gd, and Pr) have a high concentration in iron sand from the lava flow area and have a good Pearson correlation value. The combination of grain size distribution and magnetic and geochemical properties has shown differences in the characteristics of iron sand in the Tambora Volcano area.

Keywords:

iron sand, magnetic minerals, grain size, magnetic susceptibility, geochemistry, Tambora

1. Introduction

Iron sand is a type of sand that has a higher concentration of iron; the main compositions can be magnetite, ilmenite, and titanomagnetite, and it contains small amounts of silica, titanium, manganese, calcium, and vanadium (McDougall, 1961; Templeton, 2025). Iron sand is a type of titania-ferrous solution (TFSO), which is formed from the rapid cooling of volcanic lava and is widely distributed in coastal areas (Wright, 1964). Iron sand is generally found in coastal areas, rivers, and volcanic mountains with various geological settings, including magmatic arcs, volcanic islands, or continental

2021). According to Rochani et al. (2007), Indonesia

tors, including the original rock, the alteration process, the transportation media, and its deposition (Maghfiroh et al., 2023). Iron sand can come from volcanic eruptions or be formed from weathering of original rocks by weather and surface water, which are then transported and deposited along the coast or rivers (Rahmi et al., 2022). In general, iron sand deposits resulting from volcanic eruptions have a higher iron content compared to iron sand deposits resulting from weathering (Brathwaite et al., 2017; Satria et al., 2021; Zahra et al., 2023). Differences in iron type and composition can affect other properties of iron sand (Leveneur et al.,

has a large potential for iron mineral resources, consist-

arcs (Wang et al., 2015; Nugraha et al., 2016; Tiwow

et al., 2017; Satria et al., 2021; Zahra et al., 2023). The

formation of sand deposits is determined by several fac-

* Corresponding author: Putu Billy Suryanata e-mail address: putubillysuryanata@gmail.com Received: 18 December 2024. Accepted: 14 April 2025.

Available online: 21 October 2025

ing of iron sand (8%), iron ore (17%), and laterite iron ore (75%). Indonesia, with its unique geology, is home to iron sand deposits from Aceh, at the northern tip of Sumatra, to Sarmi, on the northern coast of Papua (Satria et al., 2021; Yulianto et al., 2003; Zahra et al., 2023; Kurnio, 2007; Rahmi et al., 2022). The close distance between iron sand deposits and active volcanoes indicates that most iron sand deposits originate from recent volcanic eruptions, such as on volcanic islands Sumatra, Java, Bali, the Lesser Sunda Islands, Maluku, and Papua (Rahmi et al., 2022; Nugraha et al., 2016; Togibasa et al., 2018), while iron sand deposits in Sulawesi and Papua originate from the destruction of much older rocks (Kurnio, 2007). Iron sand is one of the important elements/components for the production of steel and titanium, but its use is still limited (Leveneur et al., **2021**). In addition, iron sand can be used to replace up to 15 mass% of magnetic materials for the production of the composite magnetic without reducing its performance, thereby reducing the cost of production materials (Leveneur et al., 2021). Currently, the only country in the world that makes steel from iron sand is New Zealand (Templeton, 2025). Unfortunately, because iron sand in Indonesia has a low iron content (45-48%), so far iron sand has only been mined and used as a mixed ingredient in the production of cement and building materials (Yulianto et al., 2003; Rochani et al., 2007). This type of utilisation has low economic value. One of the iron sand deposit locations in Indonesia is on the coast around Mount Tambora, Sumbawa Island. Sumbawa Island is located in the Lesser Sunda Arc, which is a transition zone from oceanic subduction to continentisland arc collision (Darman, 2012; Minarwan, 2012). The source of iron sand in this area is likely from eruption products and from the weathering of the eruption products of Mount Tambora, which is famous for its devastating eruption in 1815 (Rampino, 1982). The eruption produced pyroclastic flows and fall deposits with a volume of more than 50 km³ (Dense-Rock Equivalent (DRE), 1.4 x 10¹⁴ kg) (Self et al., 1984; Sigurdsson and Carey, 1989; Kandlbauer and Sparks, 2014). The pyroclastic flow deposits from this eruption spread around Mount Tambora (Self et al., 1984; Abrams and Sigurdsson, 2007; Suhendro et al., 2021). In addition, the eruption products of Mount Tambora also spread to the Bengkulu region (Sumatra Island), Banda Island, and Brunei Darussalam (Kandlbauer and Sparks, **2014**). The eruption of Mount Tambora is included in the category of the largest and most powerful eruptions in history on Earth with a Volcanic Explosivity Index (VEI) of 7 (Newhall and Self, 1982; Sigurdsson and Carey, 1989; Kandlbauer and Sparks, 2014). This eruption also created a caldera with a diameter of 7 km with a depth of 1.4 km (Sutawidjaja et al., 2006) (see Figure 1). There has never been any research done on the physical and chemical characteristics of iron sand deposits from Mount Tambora. Therefore, it is important to con-

duct studies related to this at Tambora Volcano. The purpose of this study is to evaluate the geochemical, magnetic, and physical characteristics of iron sand in the Mount Tambora area. In order to accomplish this, iron sand samples were subjected to a number of measurements, such as identification of grain size distribution, magnetic susceptibility measurements, geochemical analysis (major elements and rare earth elements), and mineralogical analysis. Thus, it is expected that the results of the combination of magnetic and geochemical characteristics are used to determine the distribution of economic elements (i.e. REE) and increase the value of iron sand around Mount Tambora. By knowing the geochemical and magnetic characteristics, grain size, and sources of iron sand, it can be used as a magnetic material, and not just as a mixture in building materials.

2. Material and Methods

Field sampling was carried out in December 2018 at three locations, i.e. Nanga Miro (8° 9' 19.36" S; 117° 44' 4.45" E), Baringin Jaya (8° 17' 10.54" S; 117° 45' 32.51" E), and Hodo (8° 27' 1.44" S; 118° 4' 52.75" (see Figure 1). These sampling sites are located within the Pekat District in the Regency of Dompu, which is one of the ten regencies in the Nusa Tenggara Barat Province of Indonesia. Three samples were taken from each location so that a total of 9 samples were analysed in this study. The iron sand samples were measured in conditions without pretreatment (no grain size separation), also called bulk samples. In addition to measurements on bulk samples, a grain size sorting process was also carried out from the iron sand that was previously selected. Each sample was taken as a representative for each area. The collected samples were then prepared, and their magnetic susceptibility was measured at the Laboratory of Characterisation and Modelling of Physical Properties of Rocks, Institut Teknologi Bandung, West Java, Indonesia. Preparation began by washing the samples using running water and drying at room temperature. Furthermore, the samples were divided into 2 groups, namely the bulk sample group and the sample group for grain size analysis.

First, magnetic susceptibility measurements were carried out for all bulk samples (see **Table 1**). About 1 kg of three bulk samples from each location were set aside as bulk samples. The magnetic susceptibility is measured in a Bartington MS2 magnetic susceptibility system (Bartington Instruments Ltd., Witney, UK) with a dual frequency (470 Hz and 4.7 kHz) MS2B sensor. For this measurement, a portion of bulk was then placed inside a standard cylindrical holder (2.54 cm in diameter and 2.2 cm in height) and weighed using an Ohaus precision balance. Three holders were prepared for bulk from each location. The results of magnetic susceptibility measurements are expressed as mass-specific low and high frequency magnetic susceptibility (χ_{LF} and χ_{HF}). From the

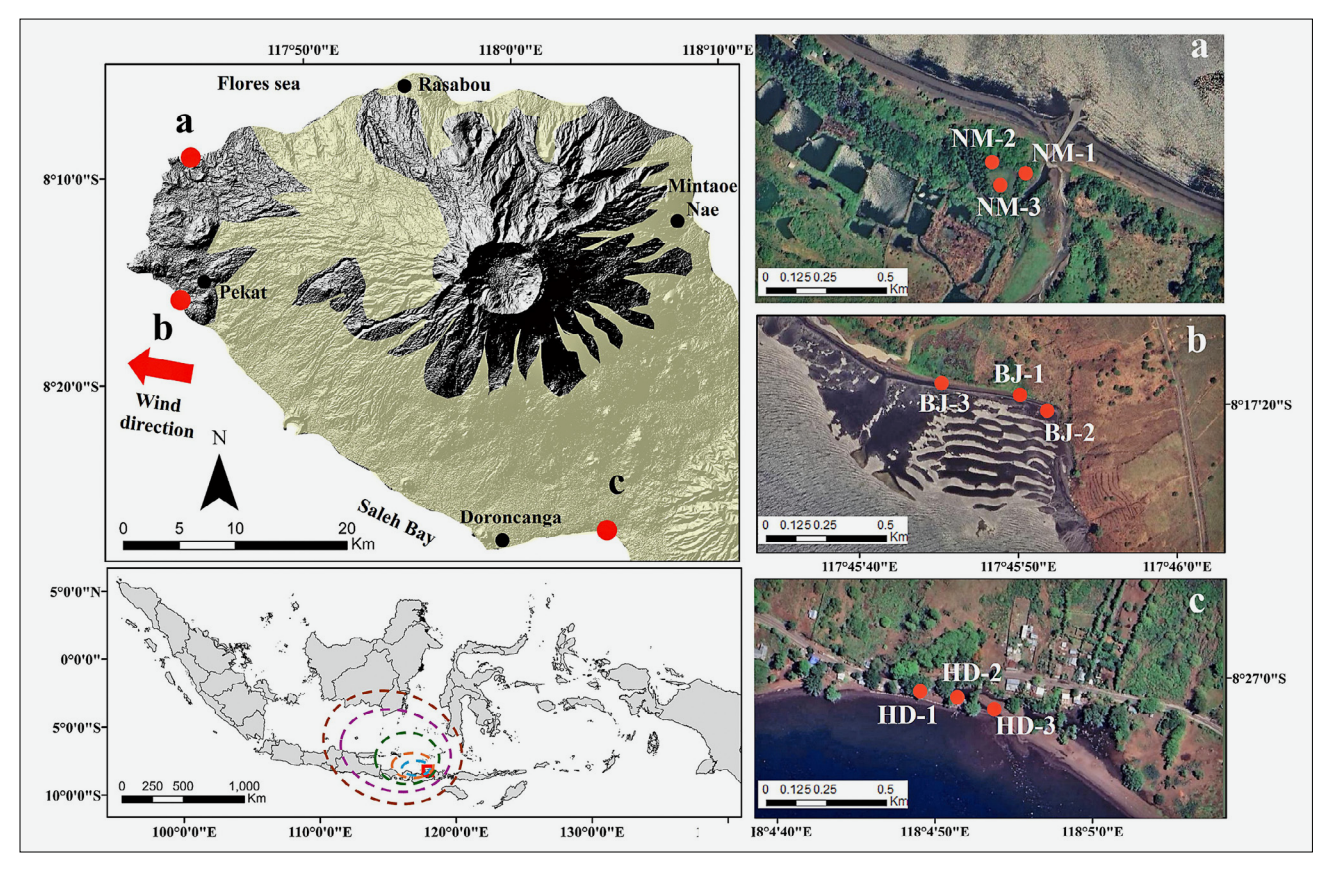


Figure 1. Sampling sites around Tambora Volcano, West Nusa Tenggara, Indonesia. Based on Sigurdsson and Carey (1989), the yellow colour shows the distribution area of pyroclastic flow around Tambora Volcano. Wind direction is indicated by the red arrow, and administrative locations are marked by the black circle. Isopach of tephra fallout (pyroclastic fall) during the 1815 eruption of Tambora based on Sigurdsson and Carey (1989) and Self et al. (1984). The isopach is symbolized by a dashed line with colour variations that indicate differences in layer thickness: blue (50 cm), orange (25 cm), green (20 cm), purple (5 cm), and brown (1 cm). There are three iron sand sampling locations shown with earth surface imagery from Google Earth (https://earth.google.com/): a) Nanga Miro, b) Baringin Jaya, and c) Hodo.

two high and low frequency values, the frequency-dependent susceptibility ($\chi_{FD\%}$) value is calculated according to Suryanata et al. (2023). Second, about 3 kg of the selected bulk samples from each location were then subjected to grain-size analyses following the Wentworth (1992) scale. The highest magnetic susceptibility value is used to determine one sample to be selected to represent each location for grain size distribution analysis. This selection was made because it was assumed that the sample with the highest susceptibility value in the same area would have a higher magnetic mineral content, and further analysis would be carried out. Samples were sieved using ASTM (American Society for Testing and Materials) standard sieves. A 10-mesh sieve was first used to eliminate particles larger than sand size. Subsequently, the samples were sieved through a series of mesh sieves. Furthermore, each result of grain size separation for different sizes will be called sub-samples. There were five sub-samples based on their grain size, i.e. very coarse sand (VCS), which has a grain size > 18 mesh; coarse sand (CS), which has a grain size between 18 and 35 mesh; medium sand (MS), which has a grain size between 35 and 60 mesh; fine sand (FS), which has a grain size between 60 and 120 mesh; and very fine sand (VFS), which has a grain size < 120 mesh. This sub-sample division refers to previous research conducted by **Satria et al. (2021)**. The sub-samples were weighed using a digital scale. Their weight percentages (mass%) were then determined by dividing their weights by the total weight before sieving. The values of mass% for the sub-samples will be referred to as grain size distribution (GSD) (see **Figure 2a**). After the grain size separation of iron sand was carried out, magnetic susceptibility measurements were carried out for all sub-samples.

Figure 2b shows the particle size distribution for selected samples. The coefficient of uniformity (CU) and the coefficient of curvature (CC) of each sub-sample could easily be calculated from the curves in **Figure 2b**. These two coefficients are defined respectively as CU = D_{60}/D_{10} and CC = $(D_{30} \times D_{30})/(D_{60} \times D_{10})$, where 10% of the particles are finer and 90% of the particles are coarser than D_{10} size, 30% of the particles are finer and 70% of the particles are coarser than D_{60} size as indicated by D_{10} , D_{30} , and D_{60} , respections

		•			-	
Sampling	g Code		Magnetic Susceptibility	XRF	XRD	REE
	BJ-1	Bulk	v			
		Bulk	v	V	v	v
		VCS	v	V	v	
Baringin	BJ-2	CS	v	V	v	
Jaya	BJ-Z	MS	v	V	v	
		FS	v	V	V	
		VFS	v	V	v	
	BJ-3	Bulk	v			
	NM-1	Bulk	v	V	V	v
		VCS	v	V	v	
		CS	v	V	V	
Nanga		MS	v	V	V	
Miro		FS	v	V	V	
		VFS	v	V	v	
	NM-2	Bulk	v			
	NM-3	Bulk	v			
		Bulk	v	V	v	v
		VCS	v	V	v	
Hodo	HD-1	CS	v	V	V	
	חט-ו	MS	v	v	v	
		FS	v	v	v	
		VFS	v	V	V	
	HD-2	Bulk	v			
	HD-3	Bulk	v			

Table 1. List of measurements on Bulk samples and sub-samples of iron sand in this study

tively (Chapuis, 2021). The values of CU for Nanga Miro, Baringin Jaya and Hodo samples are 2.32, 2.00, and 2.13, respectively, while the values of CC are 0.44, 0.40 and 0.32, respectively. Despite slight differences in their values of CU and CC, all samples could be classified as poorly graded, as expected for beach sand.

Based on the results of magnetic susceptibility measurements, we selected samples with the highest magnetic susceptibility values for the same location (NM-1, BJ-2, and HD-1) to conduct geochemical measurements (XRF and XRD) for bulk samples and all sub-samples and previous studies. We selected these samples to enable correlation with the amount of magnetic minerals. XRD analyses were carried out using a SmartLab X-Ray Diffractometer (Rigaku Corporation, Tokyo, Japan) equipped with Cu and Rigaku PDXL software (version 2.0) to identify crystal structures, lattice parameters, and perform mineral quantification. XRF analyses were carried out using a Supermini 200 X-ray fluorescence (Rigaku Corporation, Tokyo, Japan) that identifies major, minor, and trace elements contained. In this study, only the following elements were presented: Fe, Si, Ca, Al, Mg, Ti, Na, and K. The XRD and XRF measurements are conducted at the Laboratory of the Centre for Mineral and Coal Resources in Bandung, Indonesia. Furthermore, we also use the ICP-OES (Inductively Coupled Plasma Atomic-Optical Emission Spectrome-

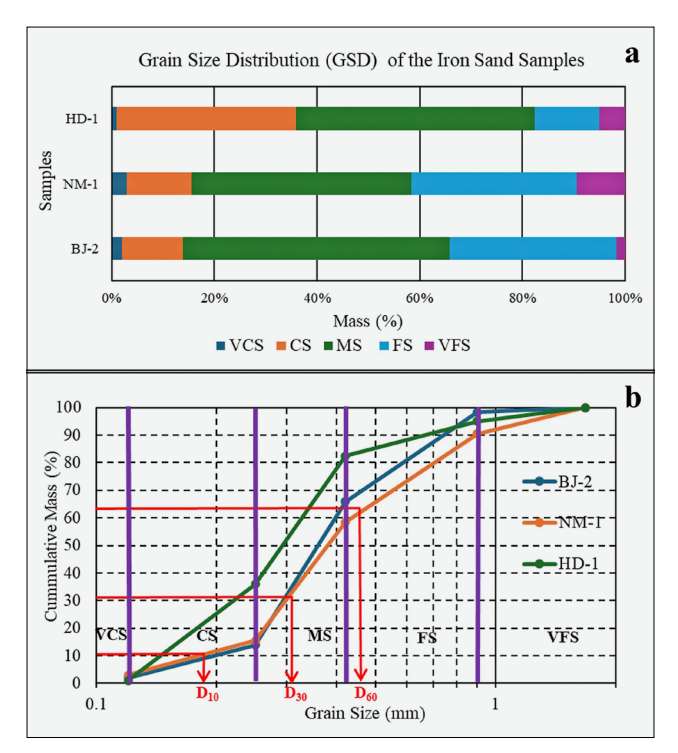


Figure 2. a) The percentage mass of iron sand grain size distribution sub-samples and b) The graph of cumulative mass of particle size distribution for selected samples. Red lines and red texts illustrate how D_{10} , D_{30} , and D_{60} were determined for samples NM-1. See text for further explanation.

try) measurement method to determine the rare earth element content contained in iron sand. In this measurement, we only use the same bulk samples as the XRF and XRD measurements. This is done to determine the REE content in the selected sample as a whole, not just at a certain grain size. This measurement used the Agilent type 700/725 (Agilent Technologies, Santa Clara, CA, USA). REE analyses were conducted at the Laboratory of the Centre for Mineral and Coal Resources in Bandung, Indonesia, that used Bushveld granite from Transvaal, South Africa, as reference material (see **Yunginger et al., 2018**). In this study, only the following elements were presented: Ce, Lu, Nd, Pr, and Gd.

3. Results

Table 2 shows the magnetic susceptibility values (χ_{LF} and $\chi_{FD\%}$) of iron sand samples from around Tambora Volcano. From **Table 2**, we can see that in general samples from the Baringin Jaya area have χ_{LF} values that are much larger than samples from Nanga Miro and Hodo, where samples from Hodo have the smallest values.

As shown in **Figure 2**, the GSD results for the BJ-2 and NM-1 samples are rather similar, while those of HD-1 are rather different. The predominant grain sizes in BJ-2 and HD-1 are MS and FS, while those in Hodo are MS and CS. In all locations, the mass% values for VCS are rather small (1 to 3%). In **Table 3**, the χ_{IF} val-

Table 2. Magnetic susceptibility of all bulk samples in three sampling locations. Bulk samples selected for grain size separation are marked in bold

Sampling Code		Bulk samples										
Sampling Code	BJ-1	BJ-2	BJ-3	NM-1	NM-2	NM-3	HD-1	HD-2	HD-3			
$\chi_{LF} (10^{-8} \text{ m}^3/\text{kg})$	5219.0	7253.2	3690.4	2670.9	2483.7	1217.9	1267.5	1037.0	1144.5			
χ _{ED} %	7.8	0.8	0.7	3.1	7.9	8.7	2.0	4.0	3.0			

Table 3. Magnetic susceptibility of sub-samples from selected bulk samples subjected to grain size separation.

	Sub-samples											
Sampling Code	VCS		CS		MS		FS		VFS			
	$\chi_{ m LF}$	$\chi_{_{\mathrm{FD}}}\%$										
BJ-2	1148.9	4.3	1459.9	0.8	5471.4	0.9	1844.4	7.5	25188.0	0.8		
NM-1	1970.8	2.3	1983.7	0.9	4766.0	0.7	1923.8	10.0	4224.6	9.7		
HD-1	1319.6	1.9	1419.6	1.5	1331.3	1.7	1054.3	3.8	1328.8	4.9		

Table 4. Results of XRF measurements of the major elements

Sample	G G:	Elements (%)									
Location	Grain Size	Fe	Si	Ca	Al	Mg	Ti	Na	K	Total	
	BJ-2 Bulk	20.7	34.1	15.1	14.7	2.2	1.9	2.5	4.7	95.9	
	BJ-2 VCS	5.4	54.4	5.2	15.9	2.4	0.6	7.3	8.5	99.6	
	BJ-2 CS	2.7	58.2	5.7	21.0	2.1	0.4	7.5	2.2	99.8	
Daningin Iora	BJ-2 MS	17.9	36.7	16.3	14.9	3.2	1.7	2.8	4.2	97.7	
Baringin Jaya	BJ-2 FS	30.4	29.8	15.0	11.9	3.6	2.5	2.1	2.3	97.6	
	BJ-2 VFS	41.5	25.1	7.6	12.2	2.0	3.6	2.3	2.7	97.0	
	Average	19.8	39.7	10.8	15.1	2.6	1.8	4.1	4.1	97.9	
	Standard Dev.	13.5	12.3	4.7	3.0	0.6	1.1	2.4	2.2	-	
	NM-1 Bulk	40.8	26.4	10.3	12.4	1.2	3.5	0.8	2.9	98.3	
	NM-1 VCS	3.4	59.4	4.4	19.7	2.4	0.5	7.6	2.3	99.8	
	NM-1 CS	1.7	58.3	6.2	26.1	1.5	0.2	4.8	1.1	99.9	
Nanga Mina	NM-1 MS	25.7	33.5	17.8	12.9	1.9	2.0	1.1	3.5	98.4	
Nanga Miro	NM-1 FS	58.4	17.4	6.5	8.6	1.6	4.7	0.5	1.1	98.8	
	NM-1 VFS	65.3	14.0	2.5	9.1	0.8	5.2	0.4	1.3	98.5	
	Average	32.6	34.8	8.0	14.8	1.6	2.7	2.5	2.0	99.0	
	Standard Dev.	24.7	18.1	5.0	6.2	0.5	1.9	2.7	0.9	-	
	HD-1 Bulk	13.5	39.3	15.9	16.1	1.2	1.1	2.3	8.0	97.4	
	HD-1 VCS	4.9	57.0	4.6	15.5	1.9	0.6	8.0	7.2	99.6	
	HD-1 CS	5.1	54.3	9.8	15.5	9.8	0.5	4.0	0.8	99.8	
Hodo	HD-1 MS	11.6	40.6	17.6	16.5	1.5	1.0	2.6	6.7	98.0	
поцо	HD-1 FS	14.6	37.8	17.0	14.2	0.7	1.4	1.4	9.6	96.7	
	HD-1 VFS	11.8	42.1	12.3	15.8	0.9	1.1	2.8	9.8	96.6	
	Average	10.2	45.2	12.9	15.6	2.6	1.0	3.5	7.0	98.0	
	Standard Dev.	3.9	7.5	4.6	0.7	3.2	0.3	2.1	3.0	-	

ues representing the magnetic susceptibility of the subsamples are listed. For BJ-2 sub-samples, the VFS has the highest χ_{LF} value, while the NM-1 sub-sample has the highest χ_{LF} value in the MS sub-sample. In all locations, finer grain sizes do not necessarily have higher χ_{LF} values and vice versa. Each location has its own pattern of the χ_{LF} values and GSD. The bulk samples as well as the VCS, CS, and MS samples from the three locations have relatively low values of $\chi_{FD\%}$ (0.7 to 4.9%), inferring the absence of SP (superparamagnetic) grains. The $\chi_{FD\%}$ values tend to be higher in finer grain sizes of FS and VFS, inferring the presence of SP grains. However, there is no clear pattern on $\chi_{FD\%}$ values with GSD. The

VFS sample from BJ-2 has the highest χ_{LF} value with a very small $\chi_{FD\%}$ value.

Geochemical test results consist of XRF, XRD, and REE measurement results. The XRF analysis for the bulk samples as well as the VCS, CS, MS, FS, and VFS sub-samples is listed in **Table 4**. The Fe content varies in bulk samples, ranging from 13.5% for HD-1 to 40.8% for NM-1. Likewise for Ti element content, NM-1 bulk samples generally have the highest Ti element content, and HD-1 samples have the lowest Ti element content (see **Figure 3**; **Table 4**). Looking into sub-samples, Fe content tends to be higher in finer grain sizes, with the exception of that in HD-1 sub-samples. The FS sub-sam-

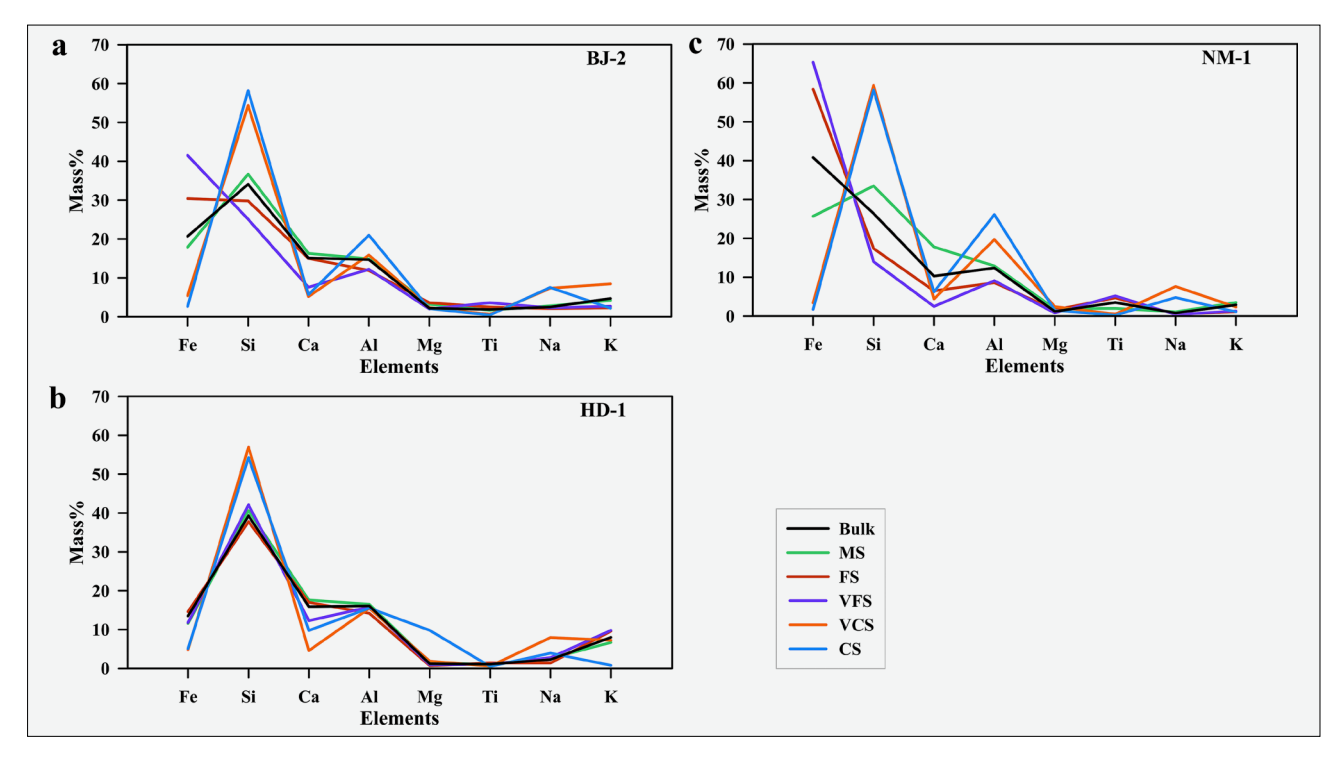


Figure 3. Element concentrations trends for bulk samples and sub-samples in three sampling locations

ple from HD-1 has higher Fe content compared to that of the VFS sub-sample. The Ti content follows the same trend as that of Fe content. However, Si content tends to be smaller in finer grain sizes, with again the exception of that in HD-1 samples. Meanwhile, Ca content consistently tends to be smaller in finer grain sizes.

The results of XRD measurements are shown in Figure 4 in the form of diffractogram patterns on bulk iron sand samples, VCS, CS, MS, FS, and VFS grain sizes. In the diffractogram of sample NM-1, it can be seen that there are magnetic minerals of the magnetite and haematite types found in bulk iron sand samples and all sub-samples. Unlike sample NM-1, in sample BJ-2 only magnetite minerals are found in all sub-samples. In the sample HD-1, there is a magnetic mineral, namely magnetite, which has a very small content. The highest magnetic mineral content is in the CS sub-sample, seen from the larger diffractogram spike (see Figure 4). All samples, bulk and sub-samples, contain labradorite and augite. Only in sample HD-1 is there analcime, and only in sample BJ-2 is there a bixbyite mineral. Overall, the results show differences in the characteristics of the three locations.

The measurement results using the ICP-OES method to test the presence of REE are listed in **Table 5**. REE concentrations are presented in the form of element concentrations in ppm. The overall results show that the concentrations of Light Rare Earth Elements (LREE) such as Ce, Gd, Nd, and Pr at all three locations are higher than the concentrations of Heavy Rare Earth Elements (HREE) such as Lu. The REE content in the NM-1 sample tends to be higher than the other two locations, where sample from the HD-1 area have the lowest REE content.

4. Discussion

The presented results show that iron sand in the Tambora Volcano area has distinctive characteristics depending on the location. These differences are observed in the distribution of grain size, magnetic susceptibility values, XRF analysis results, XRD analysis, and REE content. Magnetic susceptibility measurements for each location in the study area show a range of different χ_{IE} values. On average, the $\chi_{_{\! \rm LF}}$ values in the Baringin Jaya and Nanga Miro areas are higher than in the Hodo area (see Table 3). Variations in magnetic susceptibility values depend on the constituent minerals (Hunt et al., 1995). Based on Kartadinata et al. (2008), the rock units located around the Baringin Jaya and Nanga Miro areas are rocks from lava flows. The lava flows are products of monogenetic volcanoes that are grouped as the product of the Young Tambora Volcano (YTV) IV stage, which are predominantly lava. Another example of a group type of monogenetic volcano that is close to the Tambora Volcano is Mount Satonda. (Takada et al., 2000; Suhendro et al., 2025). Meanwhile, in the Hodo area the dominant volcanic product is the 1815 pyroclastic flow deposit consisting of a mixture of pumices, scoria, or lavas. The difference in the rocks that are the main source of eroded products that produce iron sand in the Baringin Jaya, Nanga Miro and Hodo areas causes differences in the characteristics of the minerals contained, especially magnetic minerals. The difference in magnetic minerals causes iron sand in the Baringin Jaya and Nanga Miro area to have higher susceptibility magnetic value and concentration of magnetic minerals compared

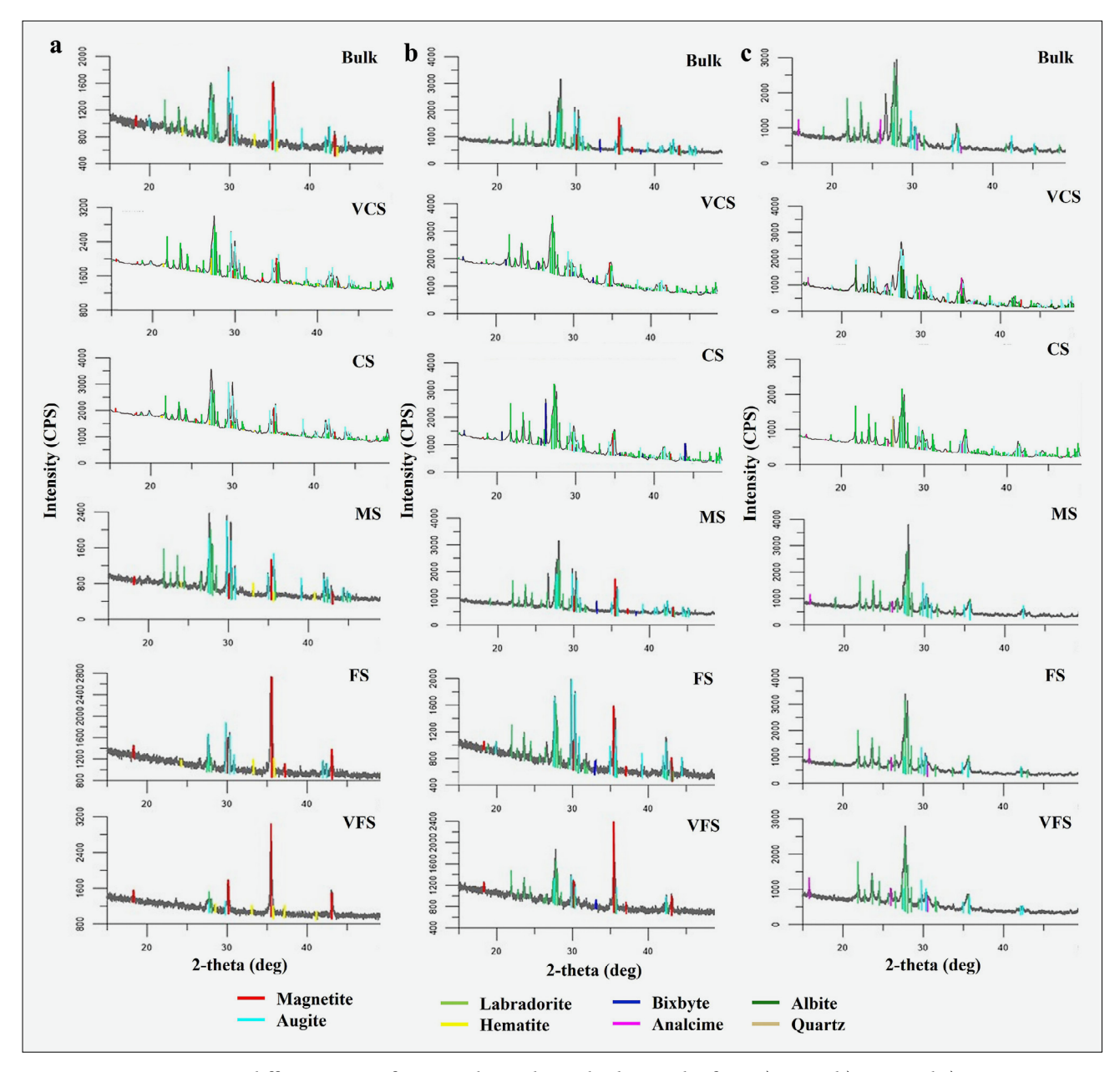


Figure 4. X-ray diffractograms of iron sand samples and sub-samples from a) NM-1, b) BJ-2, and c) HD-1.

to iron sand in the Hodo area. One of the main compositions of the 1815 Tambora pyroclastic flows is pumice, which has a fairly high SiO₂ content of around 56.5–58 mass% (Gertisser et al., 2011; Suhendro et al., 2021). Meanwhile, the lava products produced from monogenetic volcanoes are classified as basaltic and basalticandesite types (Takada et al. 2000; Kartadinata et al. 2008; Suhendro et al., 2025). Lava is usually mafic or has a low SiO₂ content, forming more magnetic minerals than pyroclastic flow, resulting in a higher magnetic susceptibility value (Pratama et al., 2018; Suhendro et al., 2021; Suryanata et al., 2023).

Samples from Nanga Miro and Baringin Jaya, which are iron sands originating from the area around the Tambora lava flow deposit, are dominated by MS and FS grain sizes. Meanwhile, the samples from the Hodo area

Table 5: The concentration of REE in bulk iron sand samples from studied locations

REE	BJ-2	NM-1	HD-1
	(ppm)	(ppm)	(ppm)
Ce	82	140	68
Gd	25	47	17
Lu	3	9	6
Nd	25	21	25
Pr	20	44	14

are iron sands originating from the area around the Tambora 1815 pyroclastic flow deposit (see **Figure 5**) and are dominated by CS and MS grain sizes. The characteristics of the grain size distribution in the Nanga Miro and

Baringin Jaya areas have the same distribution pattern as the volcanic iron sand on Lampanah Beach, Aceh (Satria et al., 2021). Genetically, the grain size distribution is closely related to wave energy in the process of washing sand grains by waves, which are then deposited (Tamuntuan et al., 2019). In addition, other elements that impact grain size distribution include terrain, transport mechanism, source material, distance from the shoreline, distance from the source (river), and transport time (Abuodha, 2003; Arens et al., 2002). From the magnetic susceptibility values of each sub-sample for each region, differences in characteristics can be seen. The VFS sub-sample has a much higher magnetic susceptibility value compared to the other sub-samples, except for the Hodo sample, which has a high magnetic susceptibility value in the CS sub-sample.

The results of the analysis of the major element content of each selected sample for the three areas show different characteristics and tend to support what is indicated by magnetic susceptibility, both for bulk samples and each sub-sample (see Tables 2, 3, and 4). Based on the concentration of Fe, the Nanga Miro and Baringin Jaya areas are those that have high concentrations compared to the Hodo area. Similar concentrations of Fe in the Nanga Miro and Baringin Jaya areas indicate that the iron sand in these areas come from the same source. This assumption is supported with geological information around the Tambora Volcano (see Figure 5). Meanwhile, the Pearson correlation value of magnetic susceptibility $(\chi_{LF} \text{ and } \chi_{FD\%})$ with major elements shows that correlation of Fe, Ti and χ_{LF} of the Baringin Jaya sample is greater than that of the other locations, while correlation of Fe, Ti and $\chi_{FD\%}$ is greater than that of the other two locations (see Table 6). The positive correlation of Fe, Ti and $\chi_{FD\%}$ and the negative correlation of Fe, Ti and χ_{LF} in the Nanga Miro sample are likely influenced by the location of the Nanga Miro iron sand sampling which is far from the rock source and vice versa for the Baringin Jaya iron sand sample, which is close to the rock source. However, the Pearson correlation for the Hodo sample does not exceed 0.75 (see **Table 6**). This indicates a different rock source of the Hodo iron sand compared to Baringin Jaya and Nanga Miro. The geochemical components of the elements and minerals contained in iron sand can be related to the Tambora eruption in 1815 and previous eruptions. The measurement results also show that iron sand in the Tambora Monogenetic lava flow (Nanga Miro and Baringin Jaya areas) has a high Fe concentration compared to iron sand in the pyroclastic flow zone, which is more felsic (higher SiO₂ content).

Based on the relationship between XRD analysis and magnetic values from the three locations, each area containing magnetic minerals has a high χ_{LF} value (Nanga Miro and Baringin Jaya). The samples from the Nanga Miro area contain a mixture of magnetite and haematite mineral content that distinguishes it from the other two locations. Magnetite is an iron oxide mineral that is

highly magnetic and sticks to magnets. Meanwhile, hematite is an iron oxide occurring in trace amounts in many natural environments with concentrations below the detection limit of many bulks' analytical techniques. The magnetic properties of hematite make it suitable for magnetic quantification, although its weak spontaneous magnetisation at room temperature (Ms=~0.4 Am² kg⁻¹) compared to magnetite (Ms=92 Am² kg⁻¹) (**Tanii** et al., 2014; Roberts et al., 2020). The presence of hematite mineral content can be one of the factors that causes the lower χ_{IE} value in iron sand from Nanga Miro area compared to Baringin Jaya area. Other characteristic minerals that are always present in all localities are labradorite and augite minerals. Both minerals are the main minerals associated with gabbro (Moghaddam et al., 2019). This shows that the type of rock in the area is mafic.

Other minerals that distinguish each region are the presence of bixbyite minerals in the Baringin Jaya area and analcime minerals in the Hodo area. Bixbyite minerals are iron-manganese oxide minerals (Rayaprol and Kaushik, 2015). They are ferrimagnetic at 300 K and antiferromagnetic at 36 K (Rayaprol et al., 2013). The magnetic properties of these minerals can contribute to the high χ_{IF} values in the Baringin Jaya area. Meanwhile, analcime minerals are a type of natural zeolite (Vereshchagina et al., 2018), which can be formed as a latestage interstitial magmatic mineral (Piper et al., 2013). This mineral consists of hydrated sodium, aluminium, and silicate. Other than magmatic, S-type (sedimentary) analcimes are authigenic minerals replacing early formed zeolites, glass of tuffs, and tuffaceous rocks (Varol, 2020). This analcime mineral is a mineral that usually characterises a deposit from pyroclastic flows (Naitza et al., 2003). It tends to have a low magnetic susceptibility value or even no magnetic properties at all. Apart from the low Fe content, this analcime content causes the susceptibility value of iron sand around the Hodo area to have a small value.

Furthermore, the REE content can be related to several other minerals from rock erosion in the area around the sample. The REE elements can come from the eruption product or weathering of rocks in the area. The concentration of LREEs such as Gd, Nd, and Pr is also found in iron sand in the Tambora Volcano area. High concentrations of LREE usually occur in sediments eroded from pyroclastic and bedrock rocks, mostly igneous rocks with alkaline types of basalt to trachyandesite (Yunginger, 2018; Gertisser et al., 2011). In placer deposits, beach sand, or heavy mineral placer deposits, REE is usually found in monazite and xenotime miner-(Gupta and Krishnamurthy, 2005; Balaram, 2019). Monazite (Ce) and monazite (Nd) minerals have paramagnetic magnetic properties (Jordens et al., 2013). The results of this study indicate that the monogenetic volcanoes lava flow has high concentrations of Ce, Gd, and Pr elements.

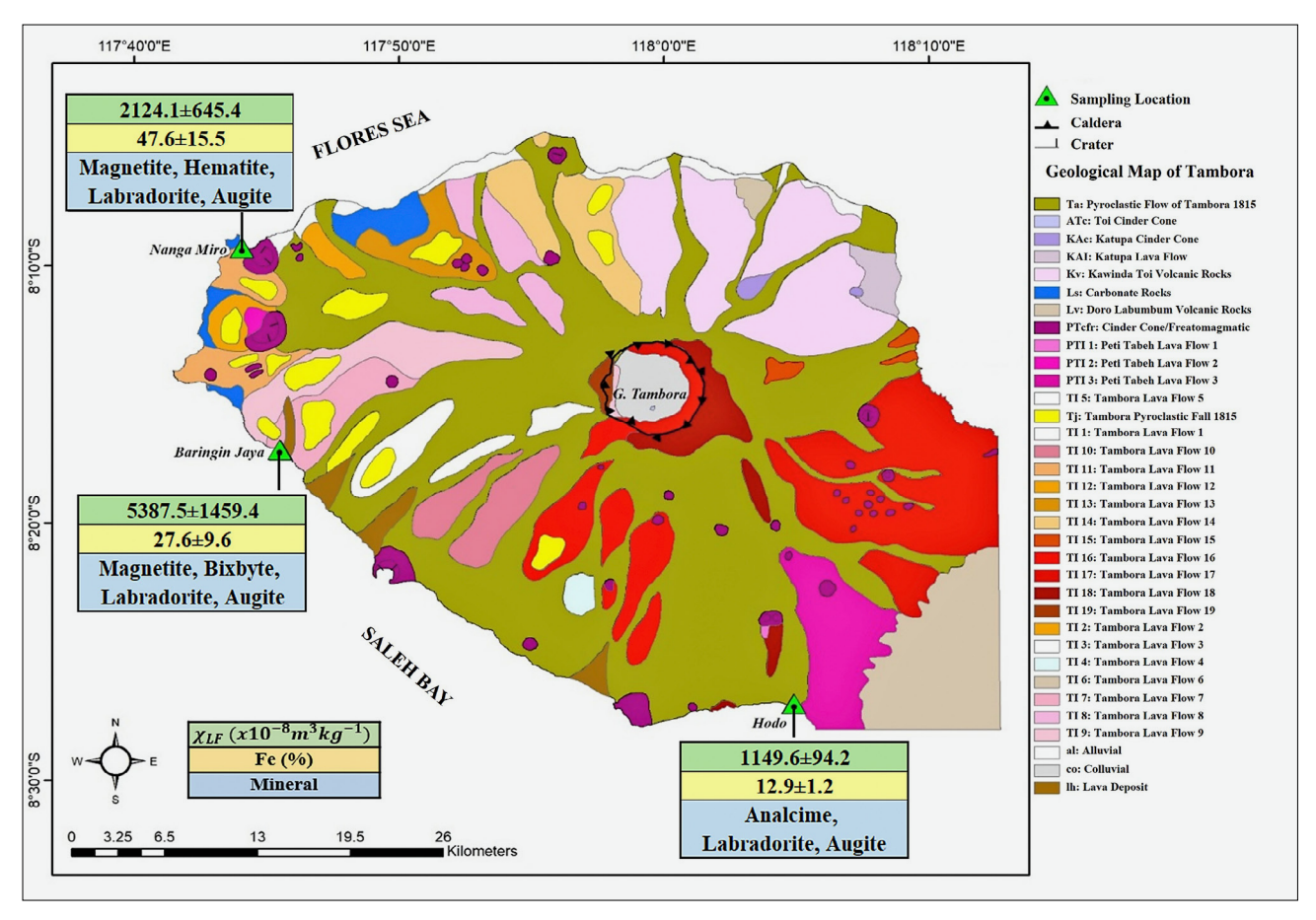


Figure 5. Geological map of the research area with research results (Modified from Kartadinata et al., 2008)

Table 6. Pearson correlation between magnetic susceptibility (χ_{LF} and $\chi_{FD\%}$) major elements for bulk samples, VCS, CS, MS, FS, and VFS sub samples for each region. Correlation value with bold format indicates positive correlation with value \geq 0.75.

Baringin Jaya Samples	χ _{FD} %	Fe	Si	Ca	Al	Mg	Ti	Na	K
$\chi_{ m LF}$	-0.43	0.77	-0.64	-0.11	-0.48	-0.40	0.81	-0.49	-0.29
χ _{FD} %		0.10	-0.08	0.12	-0.40	0.66	0.03	-0.06	0.10
Nanga Miro Samples	χ _{FD} %	Fe	Si	Ca	Al	Mg	Ti	Na	K
$\chi_{ m LF}$	-0.02	0.36	-0.47	0.52	-0.48	-0.35	0.34	-0.56	0.50
χ _{FD} %		0.85	-0.75	-0.54	-0.70	-0.48	0.85	-0.51	-0.60
Hodo Samples	$\chi_{FD}\%$	Fe	Si	Ca	Al	Mg	Ti	Na	K
$\chi_{ m LF}$	-0.30	-0.17	0.16	0.00	-0.68	0.53	-0.06	-0.17	-0.40
χ _{FD} %		0.18	-0.18	-0.08	0.20	-0.31	0.21	-0.10	0.46

We also conducted Pearson correlation between magnetic susceptibility (χ_{LF} and $\chi_{FD\%}$) and major elements with REE for bulk samples for the entire area (see **Table 7**). From **Table 7**, we can see that there is a correlation between major element concentrations and several REE elements. The element of Lu is positively correlated with $\chi_{FD\%}$ and Nd, positively correlated with Si, Ca, Al, Na, and K elements. From this, it can be seen that the erosion products of Tambora pyroclastic flow or lava flow contain fairly high REEs (Ce, Gd, and Pr) that can be associated with Fe and Ti elements. As we know, Fe and Ti are elements that form magnetic minerals, al-

though they do not have a good correlation with the magnetic susceptibility values. Further studies may be needed on the relationship between magnetic mineral characteristics from other magnetic measurements such as hysteresis parameter or remanent magnetic with geochemical analysis in iron sand.

5. Conclusions

Magnetic susceptibility and geochemical measurements combined with grain size distribution analysis resulted in a better understanding of the characteristics of

Table 7. Pearson correlation between magnetic susceptibility $(\chi_{LF} \text{ and } \chi_{FD\%})$ and major elements with REE for bulk samples for the entire area. Correlation value with bold format indicates positive correlation with value \geq 0.75.

Bulk Samples	Ce	Gd	Lu	Nd	Pr
$\chi_{ m LF}$	-0.05	0.03	-0.69	0.23	-0.04
$\chi_{\rm FD}^{0/0}$	0.62	0.56	0.98	-0.76	0.62
Fe	1.00	1.00	0.71	-0.97	1.00
Si	-0.97	-0.99	-0.59	0.92	-0.98
Ca	-1.00	-0.99	-0.79	0.99	-1.00
Al	-0.98	-0.99	-0.62	0.93	-0.98
Mg	-0.28	-0.21	-0.84	0.45	-0.28
Ti	0.99	1.00	0.67	-0.95	0.99
Na	-0.96	-0.94	-0.91	1.00	-0.96
K	-0.88	-0.91	-0.35	0.77	-0.88

iron sand along the coast around the Tambora Volcano. From three sample locations, 2 groups of different iron sand characteristics were obtained even though all three were in the Tambora Volcano area. Nanga Miro and Baringin Jaya have high magnetic susceptibility in line with high Fe element concentrations, magnetite and hematite minerals were found, higher LREE (Ce, Gd, and Pr) concentrations, and dominant grain sizes of MS and FS, while Hodo has characteristics that are the opposite of the other two areas and has grain sizes of CS and MS. Based on the concentration of Fe and magnetic minerals (iron content), it can be said that the iron sand in Hodo comes from a different source than the other samples, namely from pyroclastic flow deposit. While samples from Baringin Jaya and Nanga Miro come from lava products produced from monogenetic volcanoes of the Young Tambora Volcano (YTV) IV stage. This study also shows that the iron sand of Tambora Volcano has the potential of hosting economically valuable REEs.

Acknowledgment

The permission to conduct field research at Tambora Volcano, Dompu Regency, West Nusa Tenggara was given by the *Badan Kesatuan Bangsa dan Politik Dalam Negeri (BAKESBANGPOLDAGRI)* West Nusa Tenggara, Indonesia. Financial support for this research was provided by Education Fund Management Institution (LPDP) Indonesia through the master's degree Research Scheme to Adella Ulyandana Jayatri.

6. References

Abrams, L.J., Sigurdsson, H. (2007). Characterization of pyroclastic fall and flow deposits from the 1815 eruption of Tambora volcano, Indonesia using ground-penetrating radar. Journal of Volcanology and Geothermal Research, 161, 352–361.

- Abuodha, J.O.Z. (2003). Grain size distribution and composition of modern dune and beach sediments, Malindi Bay coast, Kenya. Journal of African Earth Sciences, 36, 41–54
- Arens, S.M., Van Boxel, J.H., Abuodha, J.O.Z. (2002):. Changes in Grain Size of Sand in Transport Over a Foredune, Earth Surface Processes and Landforms, 27, 1163 1175.
- Arsyad, M., Tiwow, V.A., Rampe, M.J. (2018). Analysis of Magnetic Minerals of Iron Sand Deposit in Sampulungan Beach Takalakar Regency South Sulawesi Using the X-Ray Diffraction Method, Journal of Physic: Conference Series, 1120, 012060.
- Balaram, V. (2019). Rare earth elements: A review of applications, occurrence, exploration, analysis, recycling, and environmental impact, Geoscience Frontiers, 10, 1285-1303.
- Brathwaite, R.L., Gazley, M.F., Christie, A.B. (2017). Provenance of Titanomagnetite in iron sand on the west coast of the North Island New Zealand, Journal of Geochemical Exploration, 178, 23-34.
- Chapuis, R.P., (2021). Analyzing grain size distributions with the modal decomposition method: literature review and procedures. Bulletin Engineering Geological Environment, 80, 6649–6666.
- Darman, H. (2012). Seismic Expression of Tectonic Features in the Lesser Sunda Islands, Indonesia. Indonesian journal of sedimentary geology, 25 (1). https://doi.org/10.51835/ bsed.2012.25.1.171
- Gertisser, R., Self, S., Thomas, L.E., Handley, H.K., Calsteren, P.V., Wolf, J.A. (2011). Processes and Timescales of Magma Genesis and Differentiation Leading to the Great Tambora Eruption 1815, Journal of Petrology, 53, 271-297.
- Gupta, C.K., Krishnamurthy, N. (2005). Extractive Metallurgy of Rare Earths. CRC Press, Boca Raton, Florida
- Hunt, C.P., Moskowitz, B.M., Banerjee, S.K. (1995). Magnetic Properties of Rock Minerals. American Geophysical Union, 189-204.
- Jordens, A., Cheng, Y.P., Waters, K.E. (2013). A review of the beneficiation of rare earth element bearing minerals. Minerals Engineering, 41, 97-114
- Kandlbauer, J., Sparks, R.S.J. (2014). New estimates of the 1815 Tambora eruption volume. Journal of Volcanology and Geothermal Research, 286, 93-100.
- Kartadinata, M.N., Mulyana, A.R., Kriswati, C., Haerani, N. (2008). Peta Geologi Gunungapi Tambora Sumbawa Provinsi Nusa Tenggara Barat, Pusat Vulkanologi dan Mitigasi Bencana Geology, Bandung. (In Indonesian Language).
- Kurnio, H., (2007). Coastal characteristics of iron sand deposits in Indonesia. Indonesia Mining Journal, 10, 27–38.
- Leveneur, J., Trompetter, W.J., Chong, S.V., Rumsey, B., Jovic, V., Kim, S., McCurdy, M., Anquillare, E., Smith, K.E., Long, N., Kennedy, J., Covic, G., Boys, J. (2021). Ironsand (Titanomagnetite- Titanohematite): Chemistry, Magnetic Properties and Direct Applications for Wireless Power Transfer. Materials, 14, 5455.
- Maghfiroh, L., Susilo, A., Wiyono, Faris, A.N. (2023). Magnetic mineral characterization of iron sand deposits in Bambang Beach Lumajang, East Java, Indonesia. International Conference on Science, Mathematics, Environment, and Education AIP Conference Proceedings, 2540.

- McDougall, J. C. (1961). Ironsand deposits offshore from the west coast North Island, New Zealand. New Zealand journal of geology and geophysics, 4, 283-300.
- Minarwan, M. (2012). Tectonic Models of the Lesser Sunda Islands. Indonesian journal of sedimentary geology, 25 (1).
- Moghaddam, M.J., Karimpour, M.H., Shafaroudi, A.M., Santos, J.F., Mendes, M.H. (2019). Geochemistry Sr-Nd isotopes and zircon U-Pb Geochronology of Intrusive Rocks: Constraint on the genesis of the Cheshmeh Khuri Cu Mineralization and its link with granitoids in the Lut Block Eastern Iran. Journal of Geochemical Exploration, 202, 59 -76.
- Naitza, S., Padalino, G., Rizzo, R. (2003). Distribution and genesis of zeolite mineralization in Cenozoic pyroclastic flows from Central Sardinia (Italy): guidelines for mineral exploration. Mineral Exploration and Sustainable Development, Milpress, Rotterdam, 915-198.
- Newhall, C. G., Self, S. (1982). The Volcanic Explosivity Index (VEI): An Estimate of Explosive Magnitude for Historical Volcanism. Journal of Geophysical Research, 87, C2, 1231-123.
- Nugraha, P.A., Sari, S.P., Hidayati, W.N., Dewi, C.R., Kusuma, D.Y. (2016). The origin and composition of iron sand deposit in the southern coast of Yogyakarta. AIP Conference Proceedings, 1746, 020028
- Piper, D. Z., Bau, M. (2013). Normalized Rare Earth Elements in Water, Sediments, and Wine: Identifying Sources and Environmental Redox Conditions, 4, 69–83.
- Pratama, A., Bijaksana, S., Abdurrachman, M., Santoso, N.A. (2018). Rock Magnetic, Petrography, and Geochemistry Studies of Lava at the Ijen Volcanic Complex (IVC), Banyuwangi, East Java, Indonesia. Geosciences, 8, 183.
- Rahmi, A., Rifai, H., Rahmayuni, R., Yuwanda, A.N., Visgun, D.A., Dwiridal, L. (2022). Irregular Magnetic Susceptibility Pattern of Iron Sand from Pasia Jambak Beach, Pasia Nan Tigo, Padang, Indonesia. Journal of Physics: Conference Series, 2309, 012027.
- Rampino, M.R. (1982). Historic Eruptions of Tambora (1815) Krakatau (1883) and Agung (1963) Their Stratospheric Aerosols and Climatic Impact, Quaternary Research, 18, 127-143.
- Rayaprol, S., Kaushik, S.D. (2015). Magnetic and Magnetocaloric Properties of FeMnO₃. Ceramics International, 8, 9567 9571.
- Rayaprol, S., Kaushik, S.D., Babu, P.D., Siguri, V. (2013). Structure and Magnetism of FeMnO₃. AIP Conference Proceeding, 1512,1132-1133.
- Roberts, A. P., Zhao, X., Hu, P., Abrajevitch, A., Chen, Y.-H., Harrison, R. J., et al. (2021). Magnetic domain state and anisotropy in hematite (α-Fe2O3) from first-order reversal curve diagrams. Journal of Geophysical Research: Solid Earth, 126, e2021JB023027.
- Rochani, S., Pramusanto, Sariman, Anugrah, R.I. (2008). The Current Status of Iron Minerals in Indonesia. Indonesian Mining Journal, 11 (11): 1-17.
- Satria, B., Masrurah, Z., Fajar, S.J. (2021). Magnetic susceptibility and grain size distribution as prospective tools for selective exploration and provenance study of iron sand deposits: A case study from Aceh, Indonesia. Heliyon 7, e08584.

- Self, S., M.R. Rampino, M.S. Newton, and J.A. Wolff, (1984).
 Volcanological study of the great Tambora eruption of 1815. Geology, 12, 659-663.
- Sigurdsson, H., Carey, S. (1989). Plinian and co-ignimbrite tephra fall from the 1815 eruption of Tambora volcano. Bulletin of Volcanology. 51: 243-270.
- Suhendro, I., Toramaru, A., Miyamoto, T., Miyabuchi, Y., Yamamoto, T. (2021). Magma chamber stratification of the 1815 Tambora caldera-forming eruption. Bulletin of Volcanology, 83: 63.
- Suhendro, I., Harijoko, A., Wibowo, H.E., Naen, G.N.R.B., Agroli, G., Nurfiani, D., Mutaqin, B.W., Sobaruddin, D.P. (2025). Timing, process, and origin of the alkaline magmas beneath Satonda volcano (Lesser Sunda Arc, Indonesia): evidence of magma mush disruption and mobilization. Bulletin of Volcanology, 87, 25.
- Suryanata, P. B., Bijaksana, S., Abdurrachman, M., Pratama, A., Desi Wulan Ndari, N. R., Fajar, S. J. (2023). Preliminary Petromagnetic Study of 1849, 1926, 1963, 1968 and 1974 Surface Lavas from Batur Volcano, Bali, Indonesia: Insight on the Magmatic Process of Source and Rock Magnetic Nature. Rudarsko-Geološko-Naftni Zbornik. 38:31–40. https://doi.org/10.17794/rgn.2023.1.3
- Sutawidjaja, I.S., Sigurdsson, H., Abrams, L. (2006). Characterization of Volcanic Deposits and Geoarchaeological Studies from the 1815 Eruption of Tambora Volcano. Jurnal Geologi Indonesia, 1, 49 57.
- Takada, A., Yamamoto, T., Kartadinata, N., Budianto, A., Munandar, A., Matsumoto, A., Suto, S., Venuti, M. C. (2000). Eruptive history and magma plumbing system of Tambora volcano, Indonesia. Report of International Research and Development Cooperation ITIT Project, Geological Survey of Japan, Philippine Institute of Volcanology and Seismology and Volcanology survey of Indonesia.
- Tamuntuan, G.H., Tanauma, A., Pasau, G., Sangian, H. (2019). Grain Size Distribution, Morphology, and Elemental Composition of Iron Sand from North Sulawesi. IOP Conference Series: Materials Science and Engineering. 567.
- Tanii, H., Inazumi, T., Terashima, K. (2014). Mineralogical Study of Iron Sand with Different Metallurgical Characteristic to Smelting with Use of Japanese Classic Iron-making Furnace Tatara, ISIJ International, 54, 1044 – 1050.
- Templeton, F. Iron and steel The steel industry, Te Ara the Encyclopedia of New Zealand, http://www.TeAra.govt.nz/en/graph/5892/chemical-composition-of-ironsands (accessed 6 March 2025 and published 12 Jun 2006)
- Tiwow, V.A., Arsyad, M., Palloan, P., Rampe, M.J. (2017). Analysis of mineral content of iron sand deposit in Bonto-kanang Village and Tanjung Bayang Beach, South Sulawesi, Indonesia. IOP Conf. Series: Journal of Physics: Conf. Series, 997, 012010.
- Togibasa, O., Bijaksana., S dan Novala, G.C. (2018). Magnetic Properties of Iron Sand from the Tor River Estuary, Sarmi, Papua. Geoscience, 8,113.
- Varol, E. (2020). Interpretation of the origin of analcimes with mineralogical, microtextural, and geochemical investigations: a case study from Aktepe region (NE of Kalecik, Ankara, Central Anatolia, Turkey). Arabian Journal of Geoscience, 13, 343.

- Vereshchagina, T.A., Kutikhina, E.A., Solovyov, L.A., Vereshchagina, S.N., Mazurova, E.V., Chernykh Y.Y., Anshits A.G. (2018). Synthesis and Structure of Analcime and Analcime Zircon Composite Derived from Coal fly ash cenospheres. Microporous and Mesoporous Materials, 258, 228-235.
- Wang, Z., Pinson, D., Chew, S., Rogers, H., Monaghan, B.J., Pownceby, M.I., Webster, N.A.S., Zhang, G. (2016). Behavior of New Zealand Ironsand During Iron Ore Sintering. Metallurgical And Materials Transactions B, 47, 330-343.
- Wentworth, C.K. (1922). A Scale of Grade and Class Terms for Clastic Sediments. The Journal of Geology, 30, 377-392.
- Wright, J.B. (1964). Iron-titanium oxides in Some New Zealand ironsands. New Zealand Journal of Geology and Geophysics, 7 (3), 424-444.

- Yulianto, A., Bijaksana, S., Loeksmanto, W. (2003). Comparative Study on Magnetic Characterization of Iron Sand from Several Locations in Central Java. Indonesian Journal of Physics, 14(2), 63.
- Yunginger, R. Bijaksana, S., Dahrin, D., Zulaikha, S., Hafidz, A., Kirana, K.H., Sudarningsih., S., Mariyanto, M., Fajar, S.J. (2018). Lithogenic and Anthropogenic Components in Surface Sediments from Lake Limboto as Shown by Magnetic Mineral Characteristics Trace Metals and REE Geochemistry, Geosciences, 8, 116.
- Zahra, H., Idrus, A., Handayani, T., Ernowo, Suwahyadi, Nugroho, D., Sunuhadi. (2023). Mineralogy and Provenance of Iron Sand Deposits from Cipatujah and Cikalong, Tasikmalaya, West Java, Indonesia. Iraqi Geological Journal, 56 (2D), 187-200.

SAŽETAK

Magnetna i geokemijska istraživanja naslaga željezovitoga pijeska oko vulkana Tambora u Sumbawi, Indonezija: alternativni pristup istraživanju visokokvalitetnoga željezovitog pijeska

Vulkan Tambora poznat je po katastrofalnoj erupciji iz 1815. godine te enormnoj količini erumpiranoga materijala piroklastičnih tokova i taloga. Procesima erozije i transporta ovi vulkanski materijali transportirani su prema obali te su formirali željezoviti pijesak koji sadržava ekonomski vrijedne minerale poput magnetita. Željezoviti pijesak jedan je od važnih elemenata/komponenti za proizvodnju čelika i titana, ali je njegova upotreba još uvijek ograničena. U Indoneziji se željezoviti pijesak vadio samo u rudnicima i koristio kao mješavina u proizvodnji cementa i građevinskih materijala zbog niskoga sadržaja željeza (Fe = 45 - 48 %). S obzirom na navedeno, važno je poznavati karakteristike i sadržaj željezovitoga pijeska kako bi se maksimizirali rezultati njegova rudarenja. Karakteristike naslaga željezovitoga pijeska s planine Tambora još uvijek su nejasne i nikada nisu proučavane. U okviru ovoga istraživanja određena su geokemijska i magnetna svojstva željezovitoga pijeska oko vulkana Tambora kako bi se dobile koncentracije ekonomskih elemenata iz različitih vulkanskih materijala. Pritom su korištena mjerenja magnetne susceptibilnosti, rendgenska difrakcijska analiza (XRD), rendgenska fluorescencijska analiza (XRF) te mjerenja spektrometrije optičke emisije u induktivno spregnutoj plazmi (ICP-OES). Uzorkovanje je obavljeno na trima lokacijama, a to su Nanga Miro, Baringin Jaya i Hodo. Nanga Miro i Baringin Jaya zone su tokova lave iz erupcije 1815. godine te tokova lave iz prethodnih erupcija, dok područje Hodo predstavlja zonu piroklastičnoga toka erupcije iz 1815. godine. Rezultati su pokazali da je raspodjela veličina zrna pijeska u Baringin Jayi i Nanga Mirou koja su iz zona tokova lave dominantno srednjih (MS) i sitnih veličina (FS). S druge strane, u području Hodo, koje je iz zone piroklastičnoga toka, zrna pijeska dominantno su krupne (CS) i srednje veličine (MS). Područja iz zona tokova lave imaju visoke vrijednosti magnetne susceptibilnosti, visoke koncentracije Fe te sadržaj magnetnih minerala magnetita i hematita. Osim toga, elementi rijetkih zemalja (Ce, Gd i Pr) imaju visoku koncentraciju u željezovitome pijesku iz područja tokova lave te upućuju na srednje vrijednosti Pearsonova koeficijenta korelacije. Kombinacija raspodjele veličine čestica te magnetnih i geokemijskih karakteristika pokazala je razlike u karakteristikama željezovitoga pijeska u području vulkana Tambora.

Ključne riječi:

željezoviti pijesak, magnetni minerali, veličina zrna, magnetni susceptibilitet, geokemija, Tambora

Author's contribution

Putu Billy Suryanata (PhD, Geophysical Engineering with expertise in rock magnetism for volcanoes) performed the field work and rock sample data collection, magnetic data measurements and processing, provided the data interpretation, composed the original draft, edited and performed project administration. Adella Ulyandana Jayatri (M.Eng., Geophysical Engineering with expertise in rock magnetism) performed the field work and rock sample data collection, magnetic data measurements and processing, provided the data interpretation, and edited the original paper. Satria Bijaksana (PhD, Professor, expert on rock magnetism) provided the rock magnetism data interpretation, edited the draft, supervision, and project administration. Silvia Jannatul Fajar (PhD, Assistant Professor, expert on rock magnetism for lakes) performed magnetic data measurements, provided rock magnetic data interpretation and proofreading. Ulvienin Harlianti (M.Eng., Geophysical Engineering with expertise on rock magnetism in lakes and palaeomagnetism) provided interpretation in rock magnetic data, wrote the original paper and proofread.

All authors have read and agreed to the published version of the manuscript.